Septin-dependent defense mechanisms against Pseudomonas aeruginosa are stalled in cystic fibrosis bronchial epithelial cells

Sylvain Brax, Clémence Gaudin, Claire Calmel, Pierre-Yves Boëlle, Harriet Corvol, Manon Ruffin, Loïc Guillot

European Journal of Cell Biology 103 (2024) 151416

Contents lists available at ScienceDirect

European Journal of Cell Biology

journal homepage: www.elsevier.com/locate/ejcb

Septin-dependent defense mechanisms against *Pseudomonas aeruginosa* are stalled in cystic fibrosis bronchial epithelial cells

Sylvain Brax [a], Clémence Gaudin [a], Claire Calmel [a], Pierre-Yves Boëlle [b], Harriet Corvol [a,c], Manon Ruffin [a], Loïc Guillot [a,*]

[a] Sorbonne Université, Inserm, Centre de Recherche Saint Antoine, Paris F-75012, France
[b] Sorbonne Université, INSERM, Institut Pierre Louis d'Épidémiologie et de Santé Publique, IPLESP, Paris F-75012, France
[c] AP-HP, Hôpital Trousseau, Service de Pneumologie Pédiatrique, Paris F-75012, France

ARTICLE INFO

Keywords:
Cystic Fibrosis
Lung
Bronchial epithelium
septins
Pseudomonas aeruginosa

ABSTRACT

Airway epithelial cells form a physical barrier against inhaled pathogens and coordinate innate immune responses in the lungs. Bronchial cells in people with cystic fibrosis (pwCF) are colonized by *Pseudomonas aeruginosa* because of the accumulation of mucus in the lower airways and an altered immune response. This leads to chronic inflammation, lung tissue damage, and accelerated decline in lung function. Thus, identifying the molecular factors involved in the host response in the airways is crucial for developing new therapeutic strategies. The septin (SEPT) cytoskeleton is involved in tissue barrier integrity and anti-infective responses. SEPT7 is critical for maintaining SEPT complexes and for sensing pathogenic microbes. In the lungs, SEPT7 may be involved in the epithelial barrier resistance to infection; however, its role in cystic fibrosis (CF) *P. aeruginosa* infection is unknown. This study aimed to investigate the role of SEPT7 in controlling *P. aeruginosa* infection in bronchial epithelial cells, particularly in CF. The study findings showed that SEPT7 encages *P. aeruginosa* in bronchial epithelial cells and its inhibition downregulates the expression of other SEPTs. In addition, *P. aeruginosa* does not regulate SEPT7 expression. Finally, we found that inhibiting SEPT7 expression in bronchial epithelial cells (BEAS-2B 16HBE14o- and primary cells) resulted in higher levels of internalized *P. aeruginosa* and decreased IL-6 production during infection, suggesting a crucial role of SEPT7 in the host response against this bacterium. However, these effects were not observed in the CF cells (16HBE14o-/F508del and primary cells) which may explain the persistence of infection in pwCF. The study findings suggest the modification of SEPT7 expression as a potential approach for the anti-infective control of *P. aeruginosa*, particularly in CF.

1. Introduction

Airway epithelial cells form a tight physical barrier against inhaled pathogens. Moreover, they coordinate the lung immune response and pathogen elimination through mucociliary clearance and the production of host defence molecules and inflammatory mediators involved in immune cell recruitment to the infection site (Whitsett and Alenghat, 2015).

People with cystic fibrosis (pwCF), a genetic disease caused by variants of the cystic fibrosis (CF) transmembrane conductance regulator (*CFTR*) gene, frequently experience lung infections caused by various microorganisms, particularly *Pseudomonas aeruginosa*, throughout the disease course (Shteinberg et al., 2021). Mucus accumulation in the lower airways and the altered immunity of pwCF favour *P. aeruginosa* infection, which persists in the lungs due to antibiotic resistance (Cohen and Prince, 2012). Associated with an exacerbated chronic inflammation and a massive neutrophil influx, this pro-inflammatory and infectious context favours lung tissue destruction

Abbreviations: CF, cystic fibrosis; CFTR, cystic fibrosis transmembrane conductance regulator; CFU, colony-forming units; DAPI, 4.6-diamidino-2-phenylindole; ETI, Elexacaftor-Tezacaftor-Ivacaftor; FCS, fetal calf serum; GAPDH, glyceraldehyde 3-phosphate dehydrogenase; GFP, green fluorescent protein; LPS, Lipopolysaccharide; PBS, phosphate buffered saline; PwCF, people with cystic fibrosis; QPCR, quantitative polymerase chain reaction; SiRNA, small interfering RNA; SEPT, septin; TSA, tryptic soy agar; TSB, tryptic soy broth.

* Corresponding author at: Inserm UMR S 938, CRSA, Bât. Kourilsky, 34 Rue Crozatier, Paris 75012, France.
E-mail addresses: sylvain.brax@inserm.fr (S. Brax), clemence.gaudin@inserm.fr (C. Gaudin), claire.calmel@inserm.fr (C. Calmel), pierre-yves.boelle@iplesp.upmc.fr (P.-Y. Boëlle), harriet.corvol@aphp.fr (H. Corvol), manon.ruffin@inserm.fr (M. Ruffin), loic.guillot@inserm.fr (L. Guillot).

https://doi.org/10.1016/j.ejcb.2024.151416
Received 29 May 2023; Received in revised form 27 March 2024; Accepted 13 April 2024
Available online 15 April 2024

and accelerates a decline in lung function, thus increasing morbidity and mortality (Shteinberg et al., 2021). Thus, identifying the molecular factors involved in the host response to infection is crucial for developing alternative and complementary strategies to antibiotics for pwCF.

P. aeruginosa is an extracellular pathogen and, therefore, does not rely on intracellular proliferation. Nevertheless, *P. aeruginosa* can invade epithelial cells using their type 6 secretion system toxins (Sana et al., 2012). However, the consequences of this internalization, particularly at the pathophysiological level, remain unclear (Muggeo et al., 2023). The first study describing the presence of intracellular *P. aeruginosa* in CF airway epithelial cells in human lung tissue has recently been shown and may explain the maintenance of chronic infection in patients (Malet et al., 2024).

The septin (SEPT) cytoskeleton is expressed in all eukaryotic cells and is involved in many cellular processes, such as tissue barrier integrity and anti-infective responses to viruses and bacteria. In humans, 13 SEPTs (SEPT1–12 and SEPT14) interact to form hetero-oligomeric complexes, non-polar filaments, and more complex structures such as rings (Ivanov et al., 2020). SEPT7 plays a critical role in maintaining the stability and function of SEPT complexes, and the knockout of SEPT7 in mice induces embryonic lethality (Menon et al., 2014). SEPTs can also detect pathogenic microbes, including the gram-negative bacterium *Shigella flexneri* (Mostowy et al., 2010). They recognize the membrane curvature of dividing bacterial cells and mediate their entrapment and delivery to lysosomes (Krokowski et al., 2018). In addition, SEPTs such as SEPT2 and SEPT9 are involved in regulating bacterial invasion, attachment, proliferation, survival, and endocytosis (Ivanov et al., 2020).

In summary, these studies suggest that SEPTs are potential candidates for improving airway epithelial cell resistance to infection in pwCFs. However, to date, investigating the role of SEPTs in infection has been restricted to the cellular level and lacks translational aspects in pathology. Furthermore, modifications to SEPT organization during *P. aeruginosa* airway infection, particularly in the context of CF, remain unknown. Here, we hypothesized that SEPT7 is involved in controlling *P. aeruginosa* infection in CF bronchial epithelial cells.

2. Material and methods

2.1. Cell and bacterial culture

BEAS-2B cells (CRL-9482™, Lot:59227035; American Type Culture Collection, Rockville, MD, USA) were cultured in F-12 medium (Invitrogen, Waltham, MA, USA) supplemented with 10 % foetal calf serum (FCS, Eurobio, Courtaboeuf, France), 10 mM HEPES (pH 7.2–7.5) and 1 % penicillin-streptomycin (Thermo Scientific, Waltham, MA, USA). Pr Dieter Gruenert (originator) and Dr Beate Illek (provider) from the University of California San Francisco generously supplied 16HBE14o- (16HBE) cells. The cells were cultured in minimum essential medium-Glutamax supplemented with 10 % FCS and 1 % antibiotics, as recommended by the manufacturer. Cells with the F508del *CFTR* variant (16HBE-CF) were obtained from the CF Foundation and cultured as recommended by the manufacturer (Valley et al., 2019). Primary human bronchial epithelial cells from healthy donors (non-CF1: batch 02AB839, age: 59, sex: male; non-CF2: batch 02AB0979, age: 36, sex: Male; non-CF3: batch 02AB68001, age: 71, sex: Female), and pwCF (CF1: batch CFAB064901, sex: female, Age: 37, F508del/1717–1 G>A; CF2: batch CFAB065301, sex: N/A, Age: N/A, F508del/c.2789+5 G>A) (Epithelix, Plan-les-Ouates, Switzerland) were cultured in a complete medium containing antibiotic (Epithelix). Cells were grown in 75 mL flasks (Techno Plastic Products, Trasadingen, Switzerland) and maintained at 37 °C in a humidified atmosphere with 5 % CO_2. Cellular infection experiments were performed in complete medium without antibiotics. The green fluorescent protein (GFP)-tagged *P. aeruginosa* PAK strain (PAK-GFP) (kindly provided by Pr Alain Filloux) was grown, as previously described (McCarthy et al., 2017). PAK-GFP was grown 16 h in tryptic soy agar (TSA) dishes (Sigma-Aldrich, Saint-Quentin Fallavier, France) at 37 °C. A colony was then isolated and cultivated in 5 mL tryptic soy broth (TSB) (Sigma-Aldrich) at 37 °C for 16 h and shaken at 120 rpm. The bacterial broth was diluted 1:100 in TSB before a 2 h 15 min culture at 37 °C and shaken at 120 rpm. Further, the bacterial broth was pelleted, rinsed with phosphate buffered saline (PBS), and resuspended in a cell culture medium devoid of antibiotics. Bacterial concentration was determined at 600 nm (OD_{600}). Lipopolysaccharide (LPS) from *P. aeruginosa* (serotype 10) and Chloroquine were from Sigma-Aldrich. Elexacaftor, tezacaftor, ivacaftor were from Selleck Chemicals (Houston, Texas, USA).

2.2. Small interfering RNA transfection

Lipofectamine™ RNAiMAX (Invitrogen) (BEAS-2B, 16HBE) or Lipofectamine 3000 (primary cells) were used for small interfering RNA (siRNA) transfection, according to the manufacturer's instructions. The cells were seeded in 12-well plates (Corning, Wiesbaden, Germany) to reach 80 % (50 % for primary cells) confluence in 24 h. They were then transfected for 72 h with 5 or 10 nM siRNA Control (CTL) (UGGUUUACAUGUUGUGUGA; Eurogentec, Seraing, Belgium), against SEPT7 (previously validated siRNA pool (Pfanzelter et al., 2018)) (5′UUGCAGCUGUGACUUAUAA3′;5′UGAAUUCACGCUUAUGGUA3′;5′-UAUGAGAACUACAGAAGCA3 ′; and 5′GCUGAGGAGAGGAGCGUA3′).

2.3. Internalization protocol

Bronchial epithelial cells were seeded in 12-well plates (Corning, Wiesbaden, Germany) and then transfected during 72 h with CTL or SEPT7 siRNA. Bacteria were then resuspended in the appropriate cell culture medium without antibiotics. The cells were then infected at various values of multiplicity of infection (MOI) for various times (see legends). After infection, the cells were washed thrice with PBS and incubated with 100 μg/mL tobramycin (Sigma-Aldrich) for 1 h, to kill all extracellular bacteria. The supernatants were stored and the cells were lysed with PBS containing 0.1 % Triton X-100. The supernatants and serial dilutions of cell lysates were plated on TSA and incubated overnight at 37 °C. Colony-forming units (CFU) were counted from cell lysate plates after verifying the complete removal of extracellular bacteria (supernatants).

2.4. Western blotting

Proteins were extracted using radioimmunoprecipitation assay buffer (Euromedex, Souffelweyersheim, France) supplemented with antiprotease-antiphosphatase (Halt™ Protease and Phosphatase Inhibitor Single-Use Cocktail; Thermo Fisher Scientific). Proteins (10 μg) were reduced and size-separated on 4–15 % Mini-PROTEAN TGX stain-free precast gels (Bio-Rad, Hercules, CA, USA) and transferred onto nitrocellulose membranes using an iBlot2 device (Thermo Fisher Scientific). Membranes were blocked with TBS-Tween 0.1 % containing 5 % non-fat dry milk. Primary antibodies were incubated for 1 h at room temperature. The following SEPT antibodies have already been validated (Pfanzelter et al., 2018): SEPT2 (60075–1, 1/20 000 Proteintech, Manchester, UK), SEPT6 (HPA005665, 1/1000, Atlas Antibody, Bromma, Sweden), SEPT7 (18991; 1/1000, IBL, Minneapolis, MN, USA), SEPT9 (A302–353A-M, 1/1000 Bethyl Laboratories, Montgomery, Texas), and SEPT11 (A304–1761-M, 1/1000, Bethyl laboratories). Glyceraldehyde 3-phosphate dehydrogenase (GAPDH) antibodies were obtained from Millipore (MAB374, 1/2000, Burlington, Massachusetts, USA). Phospho-ERK1/2 (9101; 1/1000) and total-ERK1/2 (9102; 1/1000) and LC3B (3868, 1/1000) antibodies were from Cell Signaling Technology (Danvers, Massachusetts, USA). CFTR antibody 570 (1/1000) was from Cystic Fibrosis Foundation (https://cftrantibodies.web.unc.edu). We then used horseradish peroxidase-conjugated anti--rabbit (7074, 1/5000, Cell Signalling Technology) or anti-mouse (7076,

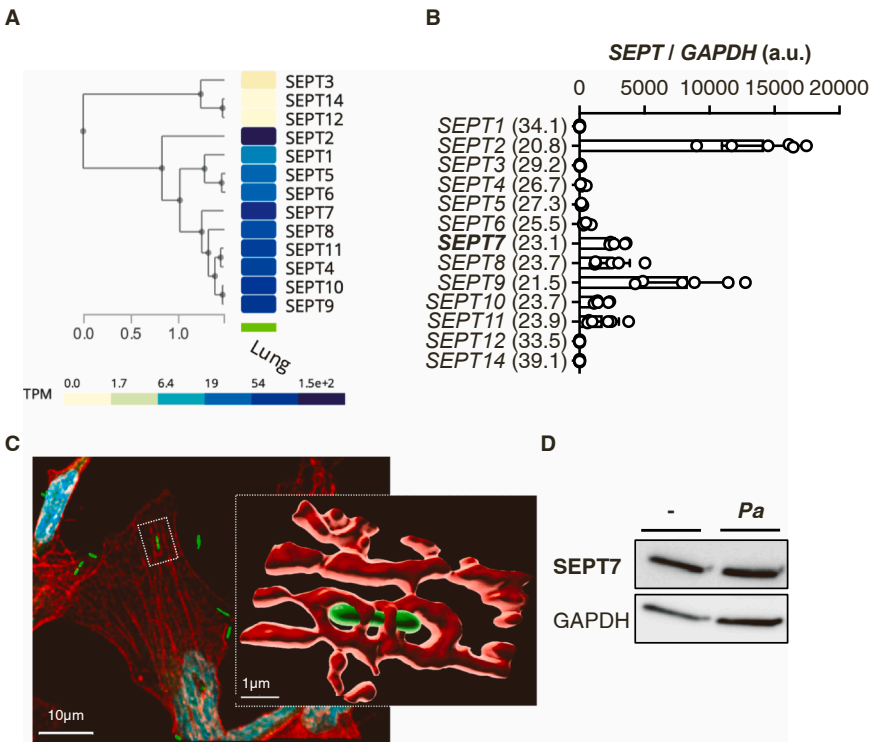

Fig. 1. (**A**) Septin (*SEPT)* transcript expressions using RNA sequencing ("RNAseq") in the lungs (public data extracted from GTEXportal.org, TPM: transcripts per million). (**B**) *SEPT* mRNA expression in BEAS-2B cells (n=6) using quantitative polymerase chain reaction (qPCR) (reference: *SEPT1,* Cycle threshold means given between brackets). (**C**) SEPT7 immunostaining (red) in BEAS-2B cells infected with *P. aeruginosa* for 3 h [multiplicity of infection (MOI) =20] (green). Nuclei are labelled with DAPI (cyan). (**D**) Western blot of SEPT7 and reference protein glyceraldehyde 3-phosphate dehydrogenase (GAPDH) in BEAS-2B cells after infecting with PAK (MOI = 5) for 3 h or not infected (NI) (representative of n= 3 experiments).

1/5000, Cell Signaling Technology) secondary antibodies, depending on the primary antibody. Detection was performed using Clarity Chemiluminescent Substrate (Bio-Rad) and images were recorded using the LAS-3000 bioimaging system (Fujifilm, Bussy-Saint-Georges, France). Densitometric quantification was performed using the ImageJ Software (https://imagej.nih.gov/ij/).

2.5. Reverse Transcription-quantitative polymerase chain reaction

RNA was extracted using the NucleoSpin RNA kit (Macherey Nagel, Düren, Germany), following the manufacturer's instructions. Reverse Transcription was performed using a high-capacity cDNA reverse transcription kit (Applied Biosystems, Foster City, CA, USA). Real-time quantitative polymerase chain reaction (qPCR) was performed using a QuantStudio 3 device (Applied Biosystems) and Sensifast Probe Lo-Rox Kit (Bio-technofix, Guibeville, France) and TaqMan probes (Applied Biosystems) for GAPDH (Hs02786624_g1), SEPT1 (Hs00364521_m1), SEPT2 (Hs01565417_m1), SEPT3 (Hs00251883_m1), SEPT4 (Hs00365352_m1), SEPT5 (Hs00954997_m1), SEPT6 (Hs00248408_m1), SEPT7 (Hs00987502_g1), SEPT8 (Hs00922332_m1), SEPT9 (Hs02246396_m1), SEPT10 (Hs00909247_g1), SEPT11 (Hs00217342_m1), SEPT12 (Hs00332566_m1), or SEPT14 (Hs01121472_m1). GAPDH was used to normalize the expression levels of the target genes. The relative expression of each gene was calculated using a reference group and the $2^{-\Delta\Delta Ct}$ method.

2.6. Immunofluorescence and confocal microscopy

Cells were seeded in 24-well plates (Corning, Corning, NY, USA) using glass coverslips. Confluent cells were infected with PAK-GFP and rinsed with PBS. The cells were fixed with 4 % paraformaldehyde for 15 min, rinsed 3× with PBS, and permeabilized (PBS containing 0.1 % Triton X-100, 10 min). Following this, the cells were incubated overnight with a blocking solution (PBS, 1 % bovine serum albumin). They were then incubated with primary SEPT7 antibody (1/100, blocking solution, 1 h at room temperature) and washed 3× with PBS. The cells were then incubated 1 h with Alexa Fluor 594 anti-rabbit secondary antibodies (Invitrogen A11012, 1/2000). The nuclei were stained with 4.6-diamidino-2-phenylindole (DAPI, Invitrogen D1306, 1/1000, PBS). Mounting and sealing were performed using ProLong mounting medium (Thermo Fisher Scientific). Standard and confocal fluorescence microscopy were performed using Olympus BX61 and Olympus FV3000 (100× oil immersion objective), respectively. Images were processed with Imaris software V9.9 (Oxford instruments, Abingdon-on-Thames, UK).

2.7. Enzyme linked immunosorbent assay

Supernatants were collected, and the interleukin (IL)-6 and IL-8 concentrations were measured using Human IL-8/CXCL8 (DY208) and Human IL-6 ELISA kits ((DY206; R&D Systems, Minneapolis, MN, USA). The substrate (3.3'5.5'-tetramethylbenzidine) was procured from Cell Signalling Technology. Absorbance was measured using a FLUOstar OPTIMA plate reader (BMG Labtech, Champigny-sur-Marne, France), and the results were analysed using MARS Data Analysis Software v3.01 R2 (BMG Labtech).

2.8. Statistical analyses

Statistical analyses were performed using GraphPad Prism 10 software. The groups were compared using the Mann–Whitney test (two groups) or ANOVA multi-comparison test with Bonferroni correction (> two groups). Statistical details, including the statistical tests and significance, have been specified in the figure legends.

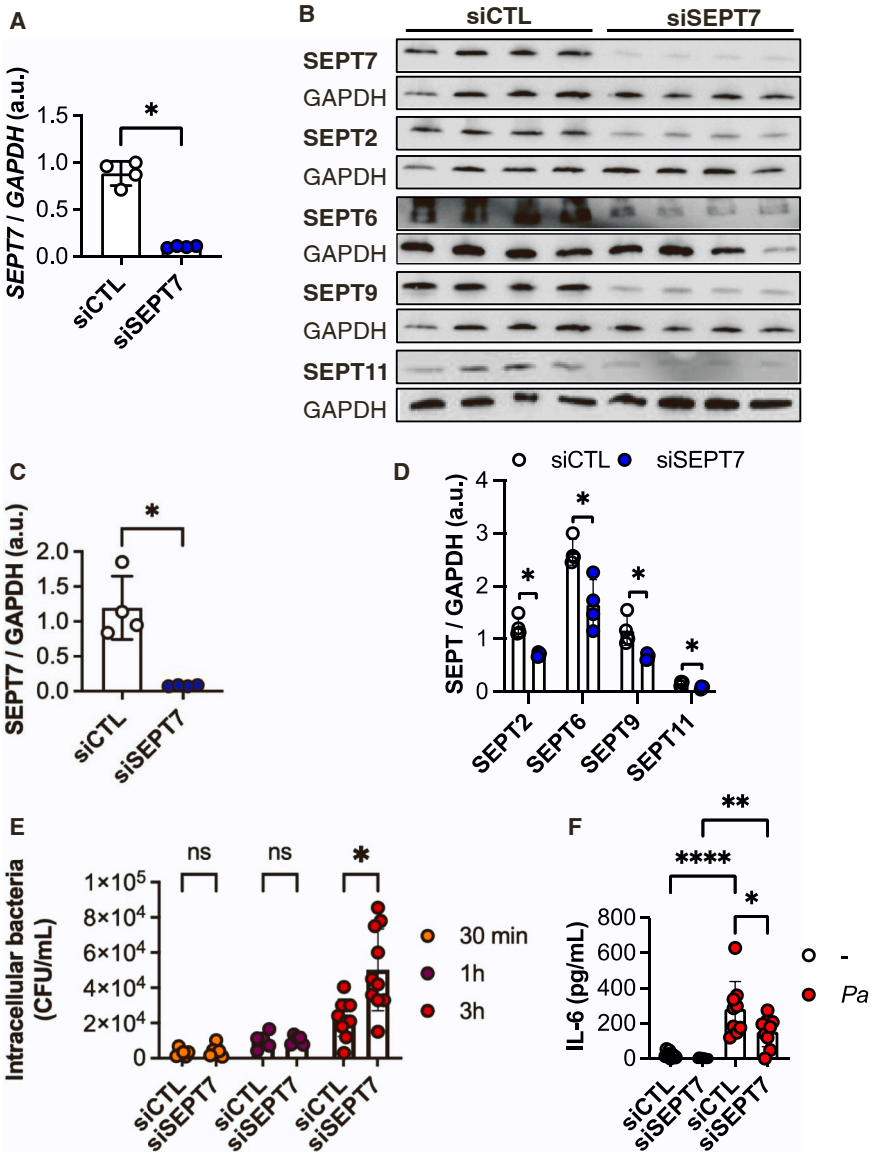

Fig. 2. *SEPT7* mRNA expression analysis using qPCR (**A**) and SEPT7 (**B**, **C**), SEPT2 (**B**, **D**), SEPT6 (**B**, **D**), SEPT9 (**B**, **D**), SEPT11 (**B**, **D**) protein expression using western blot in BEAS-2B after 72 h transfection of 5 nM control siRNA (siCTL, white circles) or SEPT7 siRNA (blue circles) (n=4, *p<0.05, Mann–Whitney test). (**E**) Amount of intracellular *P. aeruginosa* (*Pa*) (CFU/mL) in BEAS-2B cells transfected for 72 h with 5 nM of siCTL or SEPT7 siRNA and then infected for 30 min (orange circles, n=6), 1 h (purple circles, n=5) and 3 h (red circles, n=10) with *Pa* (MOI=5) [(*p<0.05, analysis of variance (ANOVA), Bonferroni correction)]. (**F**) IL-6 production by BEAS-2B cells transfected for 72 h with 5 nM of siCTL or SEPT7 siRNA in the non-infected (-, white circles) condition and after 3 h of *Pa* (red circles) infection (MOI=5) [(n= 9; *p<0.05, **p<0.01, ****p<0.0001 analysis of variance (ANOVA), Bonferroni correction)].

3. Results and discussion

To date, there are limited studies examining the specific role of SEPT in the lungs. In this study, we initially extracted the expression data of SEPT transcripts in lung tissues from a publicly available database (GTEXportal.org). Among the 13 SEPTs expressed in humans, SEPT3, SEPT12, and SEPT14 were negligibly detected in the whole lung tissue (Fig. 1 **A**). SEPT1, SEPT5, and SEPT6 were weakly expressed, whereas SEPT4, SEPT8, SEPT9, SEPT10, and SEPT11 showed intermediate expression levels. SEPT2 showed the highest expression, followed by SEPT7. Similarly, SEPT3, 12 and 14 are weakly detected in BEAS-2B cells (high Cycle threshold values). Analysis of relative SEPT expression (SEPT1 is used as a reference) in BEAS-2B cells shows that SEPT2, 9 and 7 are the three most highly expressed (Fig. 1**B**).

Intracellular bacteria with intestinal tropism, such as *S. flexneri* are internalized by HeLa epithelial cells, with 15–30 % of them being trapped in cage-like SEPT7 structures (Mostowy et al., 2010). In context of the innate immune host response, involving the key role of bronchial epithelial cells when exposed to potentially pathogenic microorganisms (Whitsett and Alenghat, 2015), we studied whether this phenomenon of encagement was also observed with a predominantly extracellular bacterium, *P. aeruginosa*, which particularly colonizes the cells of pwCF. We observed that *P. aeruginosa* was internalized in the bronchial epithelial cells of the non-cancerous BEAS-2B cell line and was found in SEPT7 structures comparable to the cages described in the literature (Fig. 1**C**). This result is consistent with recent observations in H1299 non-small cell lung cancer epithelial cells (Aigal et al., 2022). Furthermore, we did not observe any change in SEPT7 protein expression in cells infected with *P. aeruginosa* compared to uninfected cells (Fig. 1**D**).

To clarify the role of SEPT7 in the internalization of *P. aeruginosa*, we used an interfering RNA targeting *SEPT7* mRNA to downregulate its expression in BEAS-2B cells. This siRNA downregulated SEPT7 at, both, the mRNA (Fig. 2**A**) and protein levels (Figs. 2**B** and 2**C**). Consistent with several previous studies (Kinoshita et al., 2002; Lobato-Marquez et al.,

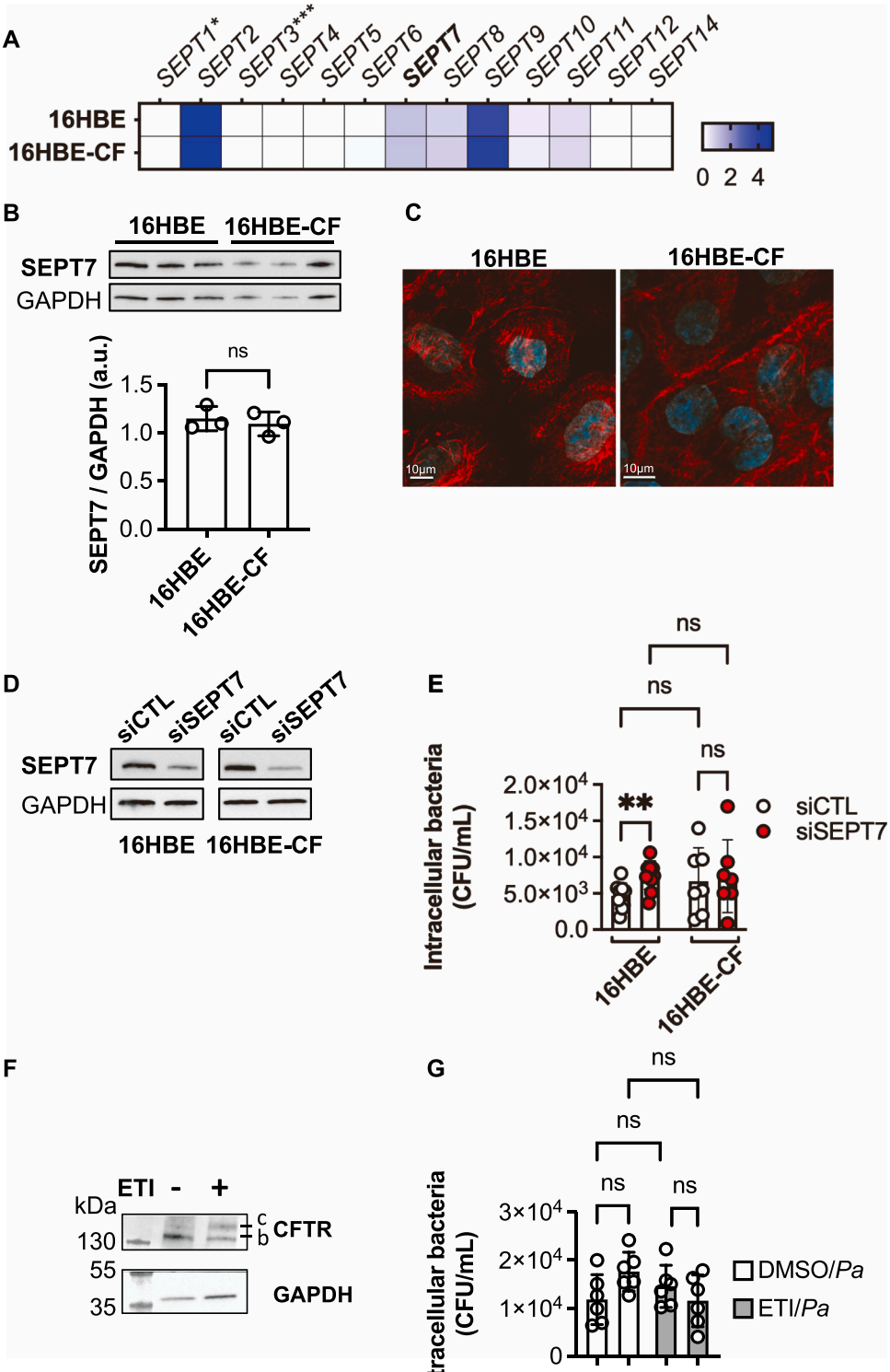

(caption on next page)

Fig. 3. (**A**) Heatmap of *SEPT* mRNA expression in 16HBE wild type (16HBE) or cystic fibrosis (16HBE-CF) cells [(n=3, *p<0.05, ***p<0.001, analysis of variance (ANOVA), Bonferroni correction)] using quantitative polymerase chain reaction (qPCR) (reference sample: 16HBE *SEPT7*). (**B**) SEPT7 protein expression analysis using western blot respectively in 16HBE or 16HBE-CF cells (n=3; ns: non-significant, Mann–Whitney test). (**C**) SEPT7 immunostaining (red) in 16HBE and 16HBE-CF cells. Nuclei are labelled with DAPI (cyan). (**D**) Western blot of SEPT7 and reference protein GAPDH in 16HBE or 16HBE-CF cells after 72 h transfection with 5 nM siCTL or SEPT7 siRNA (representative of n=4 experiments). (**E**) Amount of intracellular *P. aeruginosa* (*Pa*) (CFU/mL) in 16HBE (n=10) or 16HBE-CF (n=7) cells transfected for 72 h with 5 nM CTL or SEPT7 siRNA and then infected for 4 h with *Pa* (red circles) (MOI=10) (**p<0.01; ns: non-significant, analysis of variance (ANOVA), Bonferroni correction). (**F**) CFTR and GAPDH expression using western blot in 16HBE-CF cells incubated 72 h with vehicle (-: DMSO) or Trikafta (ETI: elexacaftor (3 μM)-tezacaftor (3 μM)-ivacaftor (1 μM)). (**G**) Amount of intracellular *P. aeruginosa* (*Pa*) (CFU/mL) in 16HBE-CF cells incubated 72 h with DMSO or ETI, transfected (24 h after ETI adding) for 48 h with 5 nM of siCTL or SEPT7 siRNA and then infected for 3 h with *Pa* (MOI=10) [(n=6; ns: not significant, analysis of variance (ANOVA), Bonferroni correction)].

2019; Pfanzelter et al., 2018; Van Ngo et al., 2022), SEPT7 inhibition reduced the protein expression of SEPT2 (Figs. 2**B** and 2**D**), SEPT6 (Figs. 2**B** and 2**D**), SEPT9 (Figs. 2**B** and 2**D**), and SEPT11 (Figs. 2**B** and 2**D**). However, this did not affect the expression of the corresponding mRNAs (**Supplementary Figure 1A**). These results confirmed that SEPT7 plays a crucial role in maintaining the SEPT cytoskeleton (Menon et al., 2014).

After infecting BEAS-2B cells with *P. aeruginosa*, an increase in the number of intracellular bacteria in cells transfected with *SEPT7* siRNA was observed (Fig. 2**E**). Nevertheless, this effect is only observable 3 h post-infection and not at shorter times. This suggests that inhibition of SEPT7 does not affect entry into the cell but rather its intracellular fate. It should also be noted that the internalization of *P. aeruginosa* was rare, accounting for approximately 2 % of the total bacteria incubated with the cells, which is consistent with data obtained from other cell lines, including MDCK (Bucior et al., 2010) and HeLa cells (Sana et al., 2012). This value reached approximately 5 % when SEPT7 expression was inhibited.

To determine whether SEPT7 inhibition altered the inflammatory response, we quantified the levels of cytokines IL-8 and IL-6, which are induced by *P. aeruginosa* in bronchial epithelial cells. No effect on IL-8 mRNA expression and protein secretion (**Supplementary Figure 1B** and **1C**) was observed under either uninfected or infected conditions. In contrast, SEPT7 inhibition significantly reduced IL-6 production following infection (Fig. 2**F**). No effect was observed on *IL-6* mRNA levels indicating that the SEPT7 inhibitory effect on IL-6 is not at the transcriptional level (**Supplementary Figure 1D**).

Interestingly, inhibition of IL-6 secretion was also observed on A549 lung epithelial cells in which septins dynamics were inhibited by forchlorfenuron and which were infected with influenza virus (Tokhtaeva et al., 2015). It has been shown that, by interacting with exocytic proteins such as soluble N ethylmaleimide-sensitive factor attachment protein receptor (SNARE) proteins, septins are required for exocytosis (Tokhtaeva et al., 2015). The difference that we observed in the effect of SEPT7 inhibition on IL-8 and IL-6 secretion might be explained by their distinct secretion mechanisms (Stanley and Lacy, 2010). Indeed, IL-6 secretion involves the SNARE protein VAMP3 (Manderson et al., 2007), whereas IL-8 secretion involves the Rho GTPases Rac1 and CDC42 (Hobert et al., 2002). However, when LPS, a *P. aeruginosa* virulence factor, is used, this decrease in IL-6 is no longer observed (**Supplementary Figure 1E**) and IL-8 remains unchanged (**Supplementary Figure 1F**). The inhibition of SEPT7 prevents the phosphorylation of ERK1/2 in the invasive breast cancer cell line, MDA-MB-231, but does not affect the p38, AKT, or JNK pathways (Zhang et al., 2016). In CF airway epithelial cells exposed to *P. aeruginosa* filtrates, IL-6 production is dependent on ERK1/2 activation (Berube et al., 2010). We did not observe that the inhibition of SEPT7 in BEAS2-B (**Supplementary Figure 2A**) or 16HBE (**Supplementary Figure 2E**) cells modulates ERK1/2 phosphorylation. All these data suggest that the decrease of IL-6 secretion is likely due to the intracellular activity (production and secretion of numerous factors) of the live bacterium. IL-6 plays a prominent role in the anti-infective response of the lungs. It also promotes epithelial repair following *P. aeruginosa* infection both *in vitro* and *in vivo* (Saint-Criq et al., 2018). Moreover, in a mouse model of acute *P. aeruginosa* infection, the administration of alveolar macrophages modified to overexpress IL-6 protected the mice from this infection and promoted lung repair (Kheir et al., 2022). Thus, reduced IL-6 levels observed *via* SEPT7 inhibition may further promote the persistence of *P. aeruginosa* within the bronchial epithelium and impair epithelial repair, a critical process in CF (Ruffin and Brochiero, 2019).

To assess the role of SEPT7 in CF, we used isogenic 16HBE and 16HBE with F508del *CFTR* variant (16HBE-F508del) cells. *SEPT* RNA expression profiles are similar (Fig. 3**A**) and SEPT7 protein expression (Fig. 3**B**) and localization (Fig. 3**C**) are identical between the two cell lines. We confirmed that SEPT7 siRNA efficiently decreased SEPT7 protein expression in both these cell types (Fig. 3**D**). We also confirmed an increase in intracellular bacteria following SEPT7 inhibition in the 16HBE bronchial cell line (Fig. 3**E**). However, this effect was not observed in 16HBE-CF cells (Fig. 3**E**). In cells expressing SEPT7, we observed a trend towards an increase in the number of intracellular bacteria in 16HBE-CF cells ($6.7\times10^3\pm4567$) compared with 16HBE cells ($4.6\times10^3\pm1704$), although without reaching significance (Fig. 3E). The variability observed in the CF group could be linked to the genomic instability of these cells and derived clones as recently demonstrated (Kerschner et al., 2023).

These results suggest an altered SEPT7 function, specific to CF. Using Elexacaftor-Tezacafor-Ivacaftor, the current therapy used in the majority of pwCF to correct CFTR expression (Fig. 3**F**) and function, we did not observe any effect on the number of intracellular bacteria (Fig. 3**G**). Thus, the altered SEPT7 function in CF cells does not seem to be directly linked to CFTR dysfunction. The CFTR-F508del mutant protein, through its interactions with numerous specific proteins (not interacting with wild-type CFTR), is associated with a wide range of cellular pathways (Lim et al., 2022; Pankow et al., 2015). Thus, the altered role of SEPT7 in CF cells might be the consequence of a disturbed cellular environment.

Septin-cage-entrapped bacteria are targeted to autophagy and SEPT7 plays a key role in eliminating bacteria, particularly *S. flexneri*, by directing them to lysosomes (Mostowy et al., 2010). Inhibition of autophagy in bronchial cells, notably by chloroquine, promotes intracellular survival of *P. aeruginosa* (Junkins et al., 2013). Furthermore, *CFTR*-mutated bronchial epithelial cells exhibit defective autophagy (Luciani et al., 2010), and ExoS, a major *P. aeruginosa* toxin, inhibits autophagy (Rao et al., 2021). These elements would favor the intracellular persistence of *P. aeruginosa* and the development of chronic colonization in patients (Flores-Vega et al., 2021). When we block autophagy with chloroquine in BEAS-2B cells, shown by induction of LC3B-II expression (**Supplementary Figure 2B**), we observed, as expected from a previous study (Junkins et al., 2013), an increase in the number of intracellular bacteria similar to that observed with inhibition of SEPT7 (**Supplementary Figure 2C**). In contrast, we observe no differences with chloroquine when SEPT7 is inhibited. Chloroquine is also able to decrease IL-6 in SEPT7 sufficient cells (**Supplementary Figure 2D**). Finally, we observed no difference in the expression of the autophagy marker LC3B between 16HBE-WT and 16HBE-CF cells (**Supplementary Figure 2E**). Thus, our data suggest that the lack of increase in intracellular bacteria observed in 16HBE-CF cells after SEPT7 inhibition is not due to a specific initial autophagic state. However, we cannot totally exclude an alteration of other specific elements of the autophagy machinery in CF cells and further work is therefore needed to understand septin-autophagy interactions during *P. aeruginosa* infection

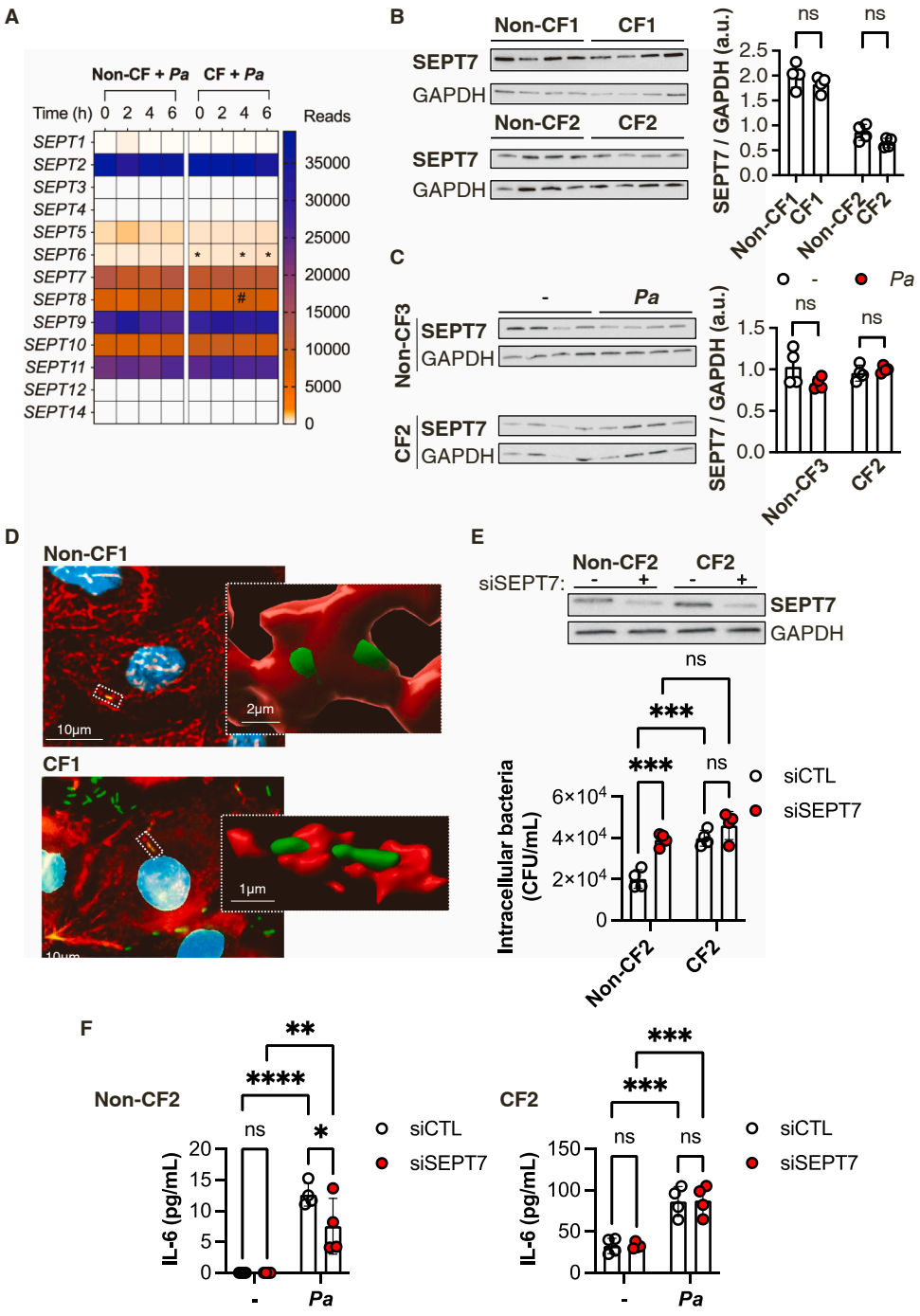

Fig. 4. (**A**) Kinetics of *SEPT* mRNA expression measured by RNAseq in primary bronchial epithelial cells from patients without CF (Non-CF, N = 4) or with CF (N = 4) and infected with *P. aeruginosa* (PAK strain, MOI 0.25) for 0, 2, 4, or 6 h (*p<0.05: CF vs. non-CF; #p<0.05: CF 4 h vs. CF 2 h, Benjamini and Hochberg corrected p-value) [data were extracted from (Balloy et al., 2015)]. (**B**) Western blot and quantification of SEPT7 and reference protein GAPDH expression in primary bronchial epithelial cells from non-CF donors (non-CF1, non-CF2) and CF patients (CF1, CF2) at baseline and (**C**) from non-CF3 and CF2 after 3 h of *Pa* infection (red circled) (MOI = 10) or non-infected (-; white circle) (n=4; ns: non-significant Mann–Whitney test). (**D**) Immunostaining of SEPT7 (red) in primary bronchial epithelial cells from non-CF1 and CF1 infected for 3 h with *Pa* (MOI=20) (green). Nuclei are labelled with DAPI (cyan). (**E**) Western blot of SEPT7 and reference protein GAPDH in Non-CF2 and CF2 cells after 96 h transfection with 10 nM siCTL or SEPT7 siRNA. Amount of intracellular *Pa* (CFU/mL) in primary non-CF2 and CF2 cells (n=6) transfected for 72 h with 10 nM CTL (white circle) or SEPT7 (red circles) siRNA and then infected for 4 h with *Pa* (MOI=10) (n=4; ***p<0.001, ANOVA, Bonferroni correction). (**F**) Interleukin-6 (IL-6) production by non-CF2 and CF2 cells transfected for 72 h with 10 nM CTL (white circle) or SEPT7 (red circle) siRNA in non-infected and after 4 h of *Pa* infection (MOI=10) (n= 4; **p<0.01, ***p<0.001, ****p<0.0001, ANOVA, Bonferroni correction).

and why SEPT7 fails to play its role in CF cells.

Knowing the limitation of 16HBE14o- cells (Kerschner et al., 2023) evocated above, we then studied primary bronchial epithelial cells. Using previous transcriptomic data (Balloy et al., 2015), we observed that *SEPT1*, 3, 4, 12 and 14 are very weakly expressed (less than 100 reads). *SEPT*5 and 6 are weakly expressed (300–1000 reads). *SEPT*7, 8 and 10 have an intermediary level of expression compared with *SEPT*2, 9 and 11, which are the most highly expressed. Overall, there were no major differences in *SEPT* expression between CF and non-CF cells. Only *SEPT*6 was significantly increased in CF cells. *P. aeruginosa* infection had

little impact on the expression of the various SEPTs. A significant increase in *SEPT8* was observed between 4 and 6 h of infection (Fig. 4**A**). We observed that SEPT7 protein is similarly expressed between primary non-CF and CF cells (Fig. 4**B**) and, as seen in BEAS-2B cells, is not regulated by *P. aeruginosa* infection (Fig. 4**C**). We also observed, both in non-CF and CF cells, bacterial encagement in SEPT7 structures comparable to those found in BEAS-2B cells (Fig. 4**D** and **Supplementary Figure 3A**). In non-CF cells, we observed, as in BEAS-2B and 16HBE cells, that inhibition of SEPT7 induces an increase of intracellular bacteria (Fig. 4**E**) associated with a decrease of IL-6 (Fig. 4**F**). Finally, similar to 16HBE-CF, SEPT7 depletion in CF primary bronchial cells did not affect the number of intracellular bacteria (Fig. 4**E**) and IL-6 level (Fig. 4**F**). IL-8 levels were not affected by SEPT7 inhibition **(Supplementary Figure 3B**). In CF cells, there are more intracellular bacteria in comparison to non-CF cells (Fig. 4**E**) and, as expected from previous data (Balloy et al., 2015), an increased inflammatory response (IL-8 and IL-6) induced by *P. aeruginosa* in CF cells than in non-CF cells (Fig. 4**F** and **supplementary Figure 3B**), which is perfectly in line with our previous results. We also observed a greater amount of IL-6 at baseline in CF cells, likely related to a constitutive activation of proinflammatory signaling directly linked to CFTR dysfunction (Cohen and Prince, 2012) (Fig. 4F).

Our results show that, although SEPT7 encages *P. aeruginosa* in CF primary cells, it does not function as expected and does not prevent the proliferation or persistence of bacteria at the intracellular level. It has recently been shown that, contrary to other bacteria, *P. aeruginosa* can be found intracellularly both in vacuoles and in the cytosol in bronchial epithelial cells (Kumar et al., 2022). Further work is required to know if this observation would be seen in CF primary bronchial epithelial cells and to understand how, in relation to SEPT7, *P. aeruginosa* could disrupt the host response according to its intracellular localization.

4. Conclusion

This study demonstrates the significance of SEPT7 in regulating *P. aeruginosa* infection and IL-6 production in bronchial epithelial cells. However, this major role was not observed in *CFTR*-deficient bronchial cells. To further elucidate CF pathology, additional investigations using differentiated primary epithelia at the air-liquid interface are required to evaluate the role of SEPT7 in *P. aeruginosa*-related pathogenicity. The study findings may potentially address whether manipulating SEPT7 expression can be considered a host-friendly strategy to promote the anti-infective control of this pathogen, particularly in the context of CF.

Funding

SB received a doctoral fellowship from the French Ministry of Higher Education, Research and Innovation. LG received grants from the French cystic fibrosis non-profit organization Vaincre la mucoviscidose (RF20220503031), Association Gregory Lemarchal and ANR (SEPT-CF, 2022-2025) to conduct the research. The Olympus FV3000 was obtained with financial support from ITMO Cancer of Aviesan within the framework of the 2021–2030 Cancer Control Strategy, on funds administered by Inserm.

CRediT authorship contribution statement

Claire Calmel: Investigation. **Pierre-Yves Boëlle:** Writing – review & editing, Funding acquisition. **Harriet Corvol:** Writing – review & editing. **Manon Ruffin:** Writing – review & editing. **Sylvain Brax:** Writing – original draft, Visualization, Validation, Methodology, Investigation, Formal analysis, Conceptualization. **Clemence Gaudin:** Methodology, Investigation, Formal analysis. **Loic Guillot:** Writing – review & editing, Writing – original draft, Visualization, Validation, Supervision, Project administration, Funding acquisition, Conceptualization.

Declaration of Competing Interest

The authors declare that they have no known competing financial interests or personal relationships that could have appeared to influence the work reported in this paper.

Data Availability

No data was used for the research described in the article.

Acknowledgements

We thank Romain Morichon and the Saint-Antoine imaging platform the for his assistance with image processing.

Appendix A. Supporting information

Supplementary data associated with this article can be found in the online version at doi:10.1016/j.ejcb.2024.151416.

References

Aigal, S., Omidvar, R., Stober, K., Ziegelbauer, J., Eierhoff, T., Schampera, J.N., Romer, W., Schwan, C., 2022. Septin barriers protect mammalian host cells against Pseudomonas aeruginosa invasion. Cell Rep. 41, 111510 https://doi.org/10.1016/j.celrep.2022.111510.

Balloy, V., Varet, H., Dillies, M.A., Proux, C., Jagla, B., Coppee, J.Y., Tabary, O., Corvol, H., Chignard, M., Guillot, L., 2015. Normal and cystic fibrosis human bronchial epithelial cells infected with pseudomonas aeruginosa exhibit distinct gene activation patterns. PLoS One 10, e0140979. https://doi.org/10.1371/journal.pone.0140979.

Berube, J., Roussel, L., Nattagh, L., Rousseau, S., 2010. Loss of cystic fibrosis transmembrane conductance regulator function enhances activation of p38 and ERK MAPKs, increasing interleukin-6 synthesis in airway epithelial cells exposed to Pseudomonas aeruginosa. J. Biol. Chem. 285, 22299–22307. https://doi.org/10.1074/jbc.M109.098566.

Bucior, I., Mostov, K., Engel, J.N., 2010. Pseudomonas aeruginosa-mediated damage requires distinct receptors at the apical and basolateral surfaces of the polarized epithelium. Infect. Immun. 78, 939–953. https://doi.org/10.1128/IAI.01215-09.

Cohen, T.S., Prince, A., 2012. Cystic fibrosis: a mucosal immunodeficiency syndrome. Nat. Med. 18, 509–519. https://doi.org/10.1038/nm.2715.

Flores-Vega, V.R., Vargas-Roldan, S.Y., Lezana-Fernandez, J.L., Lascurain, R., Santos-Preciado, J.I., Rosales-Reyes, R., 2021. Bacterial subversion of autophagy in cystic fibrosis. Front Cell Infect. Microbiol 11, 760922. https://doi.org/10.3389/fcimb.2021.760922.

Hobert, M.E., Sands, K.A., Mrsny, R.J., Madara, J.L., 2002. Cdc42 and Rac1 regulate late events in Salmonella typhimurium-induced interleukin-8 secretion from polarized epithelial cells. J. Biol. Chem. 277, 51025–51032. https://doi.org/10.1074/jbc.M210466200.

Ivanov, A.I., Le, H.T., Naydenov, N.G., Rieder, F., 2020. Novel Functions of the Septin Cytoskeleton: Shaping Up Tissue Inflammation and Fibrosis. Am J Pathol10.1016/j.ajpath.2020.09.007.

Junkins, R.D., Shen, A., Rosen, K., McCormick, C., Lin, T.J., 2013. Autophagy enhances bacterial clearance during P. aeruginosa lung infection. PLoS One 8, e72263. https://doi.org/10.1371/journal.pone.0072263.

Kerschner, J.L., Paranjapye, A., Harris, A., 2023. Cellular heterogeneity in the 16HBE14o (-) airway epithelial line impacts biological readouts. Physiol. Rep. 11, e15700 https://doi.org/10.14814/phy2.15700.

Kheir, S., Villeret, B., Garcia-Verdugo, I., Sallenave, J.M., 2022. IL-6-elafin genetically modified macrophages as a lung immunotherapeutic strategy against Pseudomonas aeruginosa infections. Mol. Ther. 30, 355–369. https://doi.org/10.1016/j.ymthe.2021.08.007.

Kinoshita, M., Field, C.M., Coughlin, M.L., Straight, A.F., Mitchison, T.J., 2002. Self- and actin-templated assembly of Mammalian septins. Dev. Cell 3, 791–802. https://doi.org/10.1016/s1534-5807(02)00366-0.

Krokowski, S., Lobato-Marquez, D., Chastanet, A., Pereira, P.M., Angelis, D., Galea, D., Larrouy-Maumus, G., Henriques, R., Spiliotis, E.T., Carballido-Lopez, R., Mostowy, S., 2018. Septins recognize and entrap dividing bacterial cells for delivery to lysosomes. e864 Cell Host Microbe 24, 866–874. https://doi.org/10.1016/j.chom.2018.11.005.

Kumar, N.G., Nieto, V., Kroken, A.R., Jedel, E., Grosser, M.R., Hallsten, M.E., Mettrucio, M.M.E., Yahr, T.L., Evans, D.J., Fleiszig, S.M.J., 2022. Pseudomonas aeruginosa can diversify after host cell invasion to establish multiple intracellular niches. mBio 13, e0274222. https://doi.org/10.1128/mbio.02742-22.

Lim, S.H., Snider, J., Birimberg-Schwartz, L., Ip, W., Serralha, J.C., Botelho, H.M., Lopes-Pacheco, M., Pinto, M.C., Moutaoufik, M.T., Zilocchi, M., Laselva, O., Esmaeili, M., Kotlyar, M., Lyakisheva, A., Tang, P., Lopez Vazquez, L., Akula, I., Aboualizadeh, F., Wong, V., Grozavu, I., Opacak-Bernardi, T., Yao, Z., Mendoza, M., Babu, M., Jurisica, I., Gonska, T., Bear, C.E., Amaral, M.D., Stagljar, I., 2022. CFTR interactome

mapping using the mammalian membrane two-hybrid high-throughput screening system. Mol. Syst. Biol. 18, e10629 https://doi.org/10.15252/msb.202110629.
Lobato-Marquez, D., Krokowski, S., Sirianni, A., Larrouy-Maumus, G., Mostowy, S., 2019. A requirement for septins and the autophagy receptor p62 in the proliferation of intracellular Shigella. Cytoskeleton (Hoboken) 76, 163–172. https://doi.org/10.1002/cm.21453.
Luciani, A., Villella, V.R., Esposito, S., Brunetti-Pierri, N., Medina, D., Settembre, C., Gavina, M., Pulze, L., Giardino, I., Pettoello-Mantovani, M., D'Apolito, M., Guido, S., Masliah, E., Spencer, B., Quaratino, S., Raia, V., Ballabio, A., Maiuri, L., 2010. Defective CFTR induces aggresome formation and lung inflammation in cystic fibrosis through ROS-mediated autophagy inhibition. Nat Cell Biol 12, 863-875, 10.1038/ncb2090.
Malet, K., Faure, E., Adam, D., Donner, J., Liu, L., Pilon, S.J., Fraser, R., Jorth, P., Newman, D.K., Brochiero, E., Rousseau, S., Nguyen, D., 2024. Intracellular Pseudomonas aeruginosa within the airway epithelium of cystic fibrosis lung tissues. Am. J. Respir. Crit. Care Med., 10.1164/rccm.202308-1451OC
Manderson, A.P., Kay, J.G., Hammond, L.A., Brown, D.L., Stow, J.L., 2007. Subcompartments of the macrophage recycling endosome direct the differential secretion of IL-6 and TNFalpha. J. Cell Biol. 178, 57–69. https://doi.org/10.1083/jcb.200612131.
McCarthy, R.R., Mazon-Moya, M.J., Moscoso, J.A., Hao, Y., Lam, J.S., Bordi, C., Mostowy, S., Filloux, A., 2017. Cyclic-di-GMP regulates lipopolysaccharide modification and contributes to Pseudomonas aeruginosa immune evasion. Nat. Microbiol. 2, 17027 https://doi.org/10.1038/nmicrobiol.2017.27.
Menon, M.B., Sawada, A., Chaturvedi, A., Mishra, P., Schuster-Gossler, K., Galla, M., Schambach, A., Gossler, A., Forster, R., Heuser, M., Kotlyarov, A., Kinoshita, M., Gaestel, M., 2014. Genetic deletion of SEPT7 reveals a cell type-specific role of septins in microtubule destabilization for the completion of cytokinesis. PLoS Genet. 10, e1004558 https://doi.org/10.1371/journal.pgen.1004558.
Mostowy, S., Bonazzi, M., Hamon, M.A., Tham, T.N., Mallet, A., Lelek, M., Gouin, E., Demangel, C., Brosch, R., Zimmer, C., Sartori, A., Kinoshita, M., Lecuit, M., Cossart, P., 2010. Entrapment of intracytosolic bacteria by septin cage-like structures. Cell Host Microbe 8, 433–444. https://doi.org/10.1016/j.chom.2010.10.009.
Muggeo, A., Coraux, C., Guillard, T., 2023. Current concepts on Pseudomonas aeruginosa interaction with human airway epithelium. PLoS Pathog. 19, e1011221 https://doi.org/10.1371/journal.ppat.1011221.
Pankow, S., Bamberger, C., Calzolari, D., Martinez-Bartolome, S., Lavallee-Adam, M., Balch, W.E., Yates, J.R., 3rd, 2015. ΔF508 CFTR interactome remodelling promotes rescue of cystic fibrosis. Nature 528, 510-516, 10.1038/nature15729.
Pfanzelter, J., Mostowy, S., Way, M., 2018. Septins suppress the release of vaccinia virus from infected cells. J. Cell Biol. 217, 2911–2929. https://doi.org/10.1083/jcb.201708091.
Rao, L., De La Rosa, I., Xu, Y., Sha, Y., Bhattacharya, A., Holtzman, M.J., Gilbert, B.E., Eissa, N.T., 2021. Pseudomonas aeruginosa survives in epithelia by ExoS-mediated inhibition of autophagy and mTOR. EMBO Rep. 22, e50613 https://doi.org/10.15252/embr.202050613.
Ruffin, M., Brochiero, E., 2019. Repair process impairment by Pseudomonas aeruginosa in epithelial tissues: major features and potential therapeutic avenues. Front Cell Infect. Microbiol 9, 182. https://doi.org/10.3389/fcimb.2019.00182.
Saint-Criq, V., Villeret, B., Bastaert, F., Kheir, S., Hatton, A., Cazes, A., Xing, Z., Sermet-Gaudelus, I., Garcia-Verdugo, I., Edelman, A., Sallenave, J.M., 2018. Pseudomonas aeruginosa LasB protease impairs innate immunity in mice and humans by targeting a lung epithelial cystic fibrosis transmembrane regulator-IL-6-antimicrobial-repair pathway. Thorax 73, 49–61. https://doi.org/10.1136/thoraxjnl-2017-210298.
Sana, T.G., Hachani, A., Bucior, I., Soscia, C., Garvis, S., Termine, E., Engel, J., Filloux, A., Bleves, S., 2012. The second type VI secretion system of Pseudomonas aeruginosa strain PAO1 is regulated by quorum sensing and Fur and modulates internalization in epithelial cells. J. Biol. Chem. 287, 27095–27105. https://doi.org/10.1074/jbc.M112.376368.
Shteinberg, M., Haq, I.J., Polineni, D., Davies, J.C., 2021. Cystic fibrosis. Lancet 397, 2195–2211. https://doi.org/10.1016/S0140-6736(20)32542-3.
Stanley, A.C., Lacy, P., 2010. Pathways for cytokine secretion. Physiology (Bethesda) 25, 218–229. https://doi.org/10.1152/physiol.00017.2010.
Tokhtaeva, E., Capri, J., Marcus, E.A., Whitelegge, J.P., Khuzakhmetova, V., Bukharaeva, E., Deiss-Yehiely, N., Dada, L.A., Sachs, G., Fernandez-Salas, E., Vagin, O., 2015. Septin dynamics are essential for exocytosis. J. Biol. Chem. 290, 5280–5297. https://doi.org/10.1074/jbc.M114.616201.
Valley, H.C., Bukis, K.M., Bell, A., Cheng, Y., Wong, E., Jordan, N.J., Allaire, N.E., Sivachenko, A., Liang, F., Bihler, H., Thomas, P.J., Mahiou, J., Mense, M., 2019. Isogenic cell models of cystic fibrosis-causing variants in natively expressing pulmonary epithelial cells. J. Cyst. Fibros. 18, 476–483. https://doi.org/10.1016/j.jcf.2018.12.001.
Van Ngo, H., Robertin, S., Brokatzky, D., Bielecka, M.K., Lobato-Marquez, D., Torraca, V., Mostowy, S., 2022. Septins promote caspase activity and coordinate mitochondrial apoptosis. Cytoskeleton (Hoboken). https://doi.org/10.1002/cm.21696.
Whitsett, J.A., Alenghat, T., 2015. Respiratory epithelial cells orchestrate pulmonary innate immunity. Nat. Immunol. 16, 27–35. https://doi.org/10.1038/ni.3045.
Zhang, N., Liu, L., Fan, N., Zhang, Q., Wang, W., Zheng, M., Ma, L., Li, Y., Shi, L., 2016. The requirement of SEPT2 and SEPT7 for migration and invasion in human breast cancer via MEK/ERK activation. Oncotarget 7, 61587–61600. https://doi.org/10.18632/oncotarget.11402.